

A fundamental plane for gamma-ray bursts with X-ray plateaus

Dainotti, M. G. ^{1,2,3}, Postnikov, S. ⁴, Hernandez, X., ⁵, Ostrowski, M. ²

July 7, 2022

ABSTRACT

A class of long Gamma-Ray Bursts (GRBs) presenting light curves with an extended plateau phase in their X-ray afterglows obeys a correlation between the rest frame end time of the plateau, T_a , and its corresponding X-ray luminosity, L_a , Dainotti et al. (2008). In this work we perform an analysis of a total sample of 176 *Swift* GRBs with known redshifts, exhibiting afterglow plateaus. By adding a third parameter, that is the peak luminosity in the prompt emission, L_{peak} , we discover the existence of a new three parameter correlation, a GRB ‘fundamental plane’. The scatter of data about this plane becomes smaller when a class-specific GRB sample is defined. This sample of 122 GRBs is selected from the total sample by excluding GRBs with associated Supernovae (SNe), X-ray flashes and short GRBs with extended emission. Moreover, we further limit our analysis to GRBs with lightcurves having good data coverage and almost flat plateaus, 40 GRBs forming our ‘gold sample’. The intrinsic scatter, $\sigma_{int} = 0.27 \pm 0.04$, for the three-parameter correlation for this last subclass is more than twice smaller than the value for the $L_a - T_a$ one, making this the tightest three parameter correlation involving the afterglow plateau phase. Finally, we also show that a slightly less tight correlation is present between L_{peak} and a proxy for the total energy emitted during the plateau phase, $L_a T_a$, confirming the existence of an energy scaling between prompt and afterglow phases.

¹Department of Physics & Astronomy, Stanford University, Via Pueblo Mall 382, Stanford CA 94305-4060, E-mail: mdainott@stanford.edu

²Obserwatorium Astronomiczne, Uniwersytet Jagielloński, ul. Orła 171, 31-501 Kraków, Poland, E-mails: dainotti@oa.uj.edu.pl, mio@oa.uj.edu.pl

³INAF-Istituto di Astrofisica Spaziale e Fisica cosmica, c/o CNR - Area della Ricerca di Bologna, Via Gobetti 101, 40129 - Bologna, Italy, E-mails: mariagiovannadainotti@yahoo.it

⁴The Center for Exploration of Energy and Matter, Indiana University, Bloomington IN 47405, USA: E-mail: postsergey@gmail.com

⁵Instituto de Astronomía, Universidad Nacional Autónoma de México, Ciudad de México 04510, México E-mail: xavier@astro.unam.mx

Subject headings: cosmological parameters - gamma-rays bursts: general, radiation mechanisms: nonthermal

1. Introduction

GRBs, the most energetic events known in astronomy with typical prompt emission energies in the 10^{53}erg range, have been detected out to redshifts of ~ 10 (Cucchiara et al. 2011). This last feature raises the tantalising possibility of extending direct cosmological studies far beyond the redshift range covered by SNe. However, it has become clear that GRBs are not standard candles in any trivial way. Indeed, the number of sub-classes into which they are grouped has grown. GRBs are classified depending on their duration into short and long (Kouveliotou et al. 1993). Later, a class of GRBs with mixed properties, such as short GRBs with extended emission, was discovered (Norris & Bonnell 2006). Among the long GRB class, depending on the value of their peak energy, GRBs can be divided into normal GRBs or X-ray Flashes (XRFs), the latter having peak energy values dimmer than the regular ones. In addition, several GRBs also present associated SNe, hereafter GRB-SNe. Regarding instead the morphology of the lightcurves, a more complex trend in the afterglow has been observed with the Swift Satellite (Gehrels et al. 2004; O’ Brien et al. 2006) showing a flat part, the plateau, soon after the steep decay of the prompt emission. Along with these categories several physical mechanisms for producing GRBs have also appeared. For example, the plateau emission has been ascribed to millisecond newborn spinning neutron stars, e.g. Zhang & Mészáros (2001), Dall’Osso et al. 2011, Bernardini et al. (2012,2013), Rowlinson et al. (2013,2014), Rea et al. (2015), to accretion onto a black hole (Cannizzo & Gerhels 2009, Cannizzo et al. 2011) or to the prior emission model (Yamazaki 2009). A promising field has been the search for correlations between the parameters describing a GRB light curve, e.g. Petrosian & Lloyd (1998), Petrosian (1999), Amati et al. (2002), Yonetoku et al. (2004), Ghirlanda et al. (2004), Cabrera et al. (2007), Ghisellini et al. (2008), Qi & Lu (2010), Oates et al. (2009), Qi et al. (2009), Willingale et al. (2010), Oates et al. (2012) to attempt their use as cosmological indicators and to glimpse insights into their nature.

The correlations thus far discovered suffer from having large scatters (Collazzi & Schaefer 2008), beyond observational uncertainties, highlighting that the events studied come from different classes of systems. As the samples of GRBs have grown over the past years, many with observed X-ray afterglows and with measured redshift, the possibility of isolating single class systems has appeared. This in turn allows to derive tighter correlations, resulting in an increase in the accuracy with which cosmological parameters can be inferred (e.g Cardone et

al. (2009, 2010), Dainotti et al. 2013b, Postnikov et al. 2014), and yielding more stringent class specific constraints on physical models describing them.

One of the first attempts to standardize GRBs in the afterglow parameters was presented in Dainotti et al. (2008,2010) where a correlation between the rest frame end time of the plateau phase, T_a (in our previous papers T_a^*), and its corresponding luminosity L_a was discovered, hereafter the $L_a - T_a$ correlation. This correlation shows that T_a and L_a are approximately inversely proportional. Further studies, e.g. (Dainotti et al. 2011a) have shown the possibility to use the $L_a - T_a$ correlation as a redshift estimator and as an indicator of the ratio between GRB rate and star formation rate (Dainotti et al. 2015a). In addition, Dainotti et al. (2013a) has shown through the robust statistical Efron & Petrosian (1992) method, that this correlation is intrinsic, and not an artefact of selection effects or detection thresholds, as is also the case for the $L_{peak} - L_a$ correlation, (Dainotti et al. 2011b,2015b), where L_{peak} is the peak luminosity in the prompt emission.

In this letter we show how a careful discrimination of plateau phase GRBs can be performed to isolate, using X-ray afterglow light curve morphology, a sub class of events which define a very tight plane in a three dimensional space of $(\log L_a, \log T_a, \log L_{peak})$. A three parameter correlation emerges with a scatter of 24% less than the $L_a - T_a$ correlation for the sample of 122 long GRBs. When we choose a class specific subsample of high quality data (40 GRBs, hereafter the gold sample), a further 38% reduction in the scatter appears. We note that the intrinsic scatter of the $L_a - T_a - L_{peak}$ correlation for the gold sample is 54% smaller than the scatter of the $L_a - T_a$ correlation for the 122 long GRB sample. A slightly more scattered $L_{peak}, (L_a T_a)$ correlation is also present, which together with an almost constant total energy within the plateau phase for the gold sample is indicative of a strong energy coupling between the prompt emission and the X-ray afterglow phase. In section §2 we describe the *Swift* data sample used, in section §3 we present the three parameter correlation. In section §4 we present the $(L_a T_a, L_{peak})$ correlation as the tightest currently available involving the afterglow phase, together with our concluding remarks.

2. Sample selection

We analysed the sample of all 176 GRB X-ray plateau afterglows detected by *Swift* from January 2005 up to July 2014 with known redshifts, spectroscopic or photometric, available in Xiao & Schaefer (2009), in the Greiner web page ¹ and in the Circulars Notice (GCN). We exclude GRBs with redshifts for which there is only a lower or an upper limit in their

¹<http://www.mpe.mpg.de/jcg/grbgen.html>

determination. The redshift range of our sample is (0.033, 9.4). We include all the X-ray plateaus for which the afterglow light curves can be fitted by the Willingale et al. (2007), phenomenological model, hereafter W07. The W07 functional form for $f(t)$ is:

$$f(t) = \begin{cases} F_i \exp\left(\alpha_i \left(1 - \frac{t}{T_i}\right)\right) \exp\left(-\frac{t_i}{t}\right) & \text{for } t < T_i \\ F_i \left(\frac{t}{T_i}\right)^{-\alpha_i} \exp\left(-\frac{t_i}{t}\right) & \text{for } t \geq T_i \end{cases} \quad (1)$$

for both the prompt (index ‘i=p’) γ -ray and initial X-ray decay and for the afterglow (“i=a”), modeled so that the complete lightcurve $f_{tot}(t) = f_p(t) + f_a(t)$ contains two sets of four parameters $(T_i, F_i, \alpha_i, t_i)$. The transition from the exponential to the power law occurs at the point $(T_i, F_i e^{-t_i/T_i})$ where the two functional forms have the same value. The parameter α_i is the temporal power law decay index and the time t_i is the initial rise timescale. In previous papers such as W07 and Dainotti et al. (2008,2010) the *Swift* Burst Alert Telescope (BAT)+ X-Ray Telescope (XRT) lightcurves of GRBs were fitted to Eq. (1) assuming that the rise time of the afterglow, t_a , started at the time of the beginning of the decay phase of the prompt emission, T_p , namely $t_a = T_p$. Here we relax this assumption leaving t_a free. We exclude the cases which are not well fitted by the W07 model, namely when the fitting procedure fails or when the determination of 1σ confidence intervals does not fulfill the Avni (1976) χ^2 prescriptions, for more details see the xspec manual². We compute the source rest-frame luminosity L_a in units of *erg/s* in the *Swift* XRT band pass, $(E_{min}, E_{max}) = (0.3, 10)$ keV as follows:

$$L_a = 4\pi D_L^2(z) F_X(E_{min}, E_{max}, T_a) \cdot K, \quad (2)$$

where $D_L(z)$ is the GRB luminosity distance for the redshift z , computed assuming a flat Λ CDM cosmological model with $\Omega_M = 0.3$ and $H_0 = 70 \text{ km s}^{-1} \text{ Mpc}^{-1}$, F_X is the measured X-ray energy flux in (*erg/cm*²*s*⁻¹) and K is the K -correction for cosmic expansion $(1+z)^{(\alpha-1)}$. The lightcurves are taken from the Swift web page repository, http://www.swift.ac.uk/burst_analyser and we followed Evans et al. (2009) for the evaluation of the spectral parameters. As shown in Dainotti et al. (2010) requiring a homogeneous sample also implies removing short GRBs with extended emission from the analysis. In addition, as pointed out in Dainotti et al. (2016a), there is a difference in the slope of the $L_a - T_a$ correlation between GRB-SNe and long GRBs with no associated SNe, therefore in

²<http://heasarc.nasa.gov/xanadu/xspec/manual/XspecSpectralFitting.html>.

the interest of selecting a homogeneous class of objects, we decided to consider only the long GRBs with no associated SNe. Similarly, since 12 GRBs are common to the GRB-SNe and XRFs samples, we removed from our analysis all XRFs as well. Figure 1 shows the light curve for GRB 061121 with the best fit model light curve superimposed. The plateau phase is clearly seen between 2.6 and 3.8 in $\log(T)$ in units of seconds (s).

In all that follows L_{peak} is defined as the prompt emission peak flux over a 1 s interval, in units of erg/s . Following Schaefer (2007) we compute L_{peak} as follows:

$$L_{peak} = 4\pi D_L^2(z) F_{peak}(E_{min}, E_{max}, T_a) \cdot K, \quad (3)$$

where F_{peak} is the measured gamma-ray energy flux over a 1 s interval ($ergcm^{-2}s^{-1}$). To make the sample for this analysis more homogeneous also from the point of view of the spectral features, we consider only the GRBs for which the spectrum computed at 1 second, the peak flux, has a smaller χ^2 for a single power law (PL) fit than for a cut off power law (CPL). More specifically, we follow the criterion of Sakamoto et al. (2010) according to which when the $\chi_{CPL}^2 - \chi_{PL}^2 < 6$, the PL fit is preferred. We also discard 6 additional GRBs which were better fitted with a Black Body model than with a PL. The full set of class specific criteria described above leave us with a sample of 122 long GRBs. Finally, we construct a sub sample by including strict data quality and morphology criteria: that the plateau is not too steep (the angle of the plateau is smaller than 41 degrees) and that there are at least 5 points at its beginning. This last data quality cut defines the gold sample, which includes 40 GRBs. We have also checked through the T-test that this gold sample is drawn from the same distribution of (L_a, T_a, L_{peak}, z) as the full sample, thus showing that the choice of this particular sample does not introduce any biases, such as the Malmquist or Eddington ones, against high luminosity and/or high redshift GRBs.

3. The (L_a, T_a, L_{peak}) parameter space

The left panel of figure (2) shows the 176 sample in the (L_a, T_a, L_{peak}) parameter space, where we see that distinct sub-classes of GRBs show greater spread about the plane than the gold sample we have defined. The right panel in figure (2) shows the fundamental plane in projection for the 122 long GRBs, the reduction in the intrinsic scatter is clear.

To further explore if the two-dimensional $L_a - T_a$ correlation is the projection of a tighter $(L_a - T_a - L_{peak})$ plane, we plot the 122 long GRBs, in a (L_a, T_a) plane, binned according to their L_{peak} values into three equally populated ranges : $49.9 \leq \log L_{peak} \leq 51.4$, $51.4 \leq \log L_{peak} \leq 51.8$, $51.8 \leq \log L_{peak} \leq 53.0$, red circles, blue squares and black triangles,

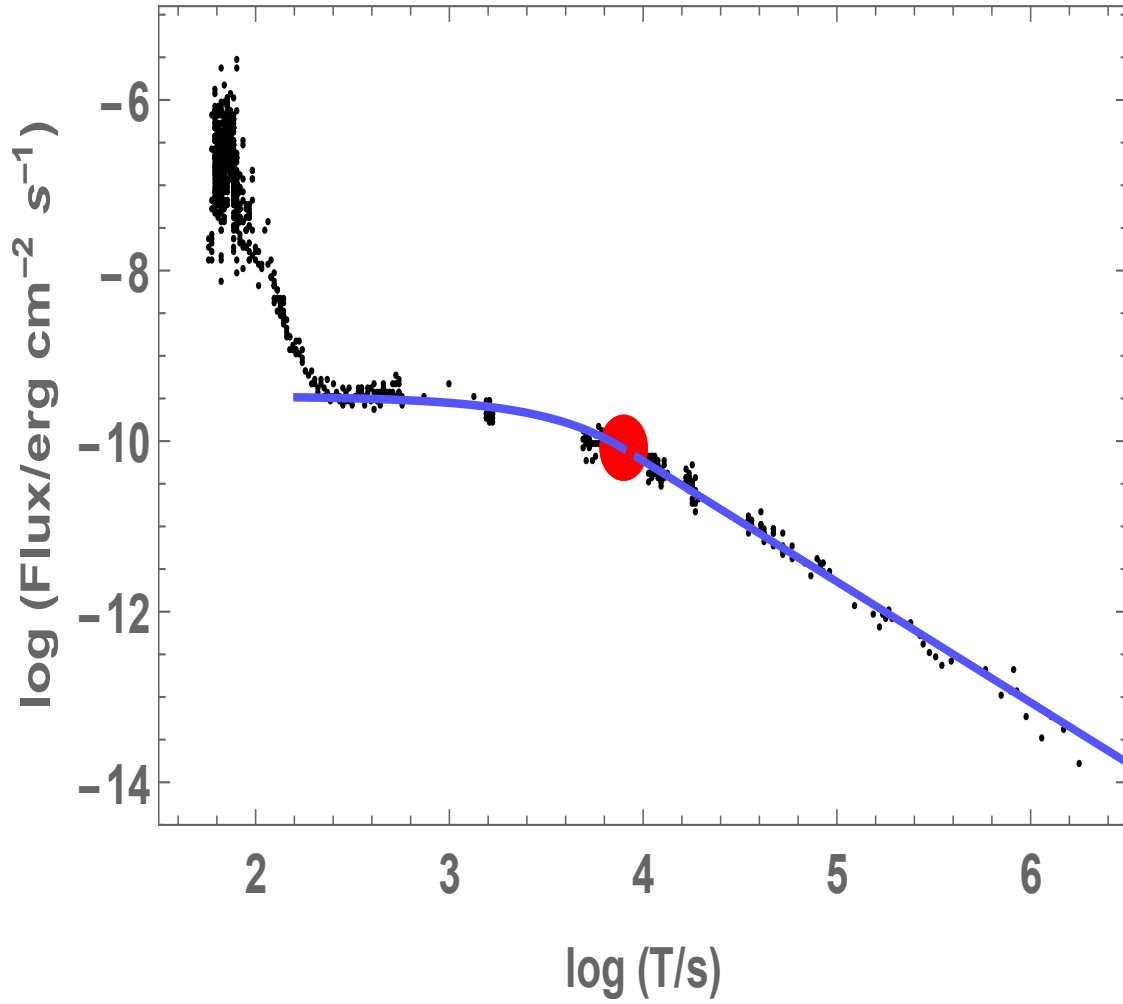


Fig. 1.— An example of the observed light curve for GRB 061121 with the best fit W07 model superimposed. Time, T , is given in the observer frame in seconds, the red dot marks the end of the plateau phase in the X-ray afterglow.

respectively, in the left panel of figure (3). For references, the curves show best fit lines of fixed slope equal to one and free intercept calculated for each L_{peak} bin. We see a clear monotonic trend, in that the intercept of the lines is determined by the L_{peak} bin of the subsample, all of which show a significantly smaller dispersion than the 122 GRB sample. The above is indicative of a fundamental plane in the (L_a, T_a, L_{peak}) parameter space, the well-known $L_a - T_a$ correlation being just a projection of a more fundamental three dimensional plane.

Parametrizing this planes using the angles θ and ϕ of its unit normal vector gives:

$$\log L_a = C_o - \cos(\phi) \tan(\theta) \log T_a - \sin(\phi) \tan(\theta) \log L_{peak}, \quad (4)$$

where $C_o = C(\theta, \phi, \sigma_{int}) + z_o$ is the normalization of the plane correlated with the other variables, θ, ϕ and σ_{int} ; while z_o is the uncorrelated fitting parameter related to the normalization and C is the covariance function. This normalization of the plane allows the resulting parameter set, $\theta, \phi, \sigma_{int}$ and z_o to be uncorrelated and provides explicit error propagation. Now we study the distribution of the 40 gold sample GRBs in the (L_a, T_a, L_{peak}) parameter space. Carefully accounting for all the error propagation we fit an optimal plane for this distribution given by:

$$\log L_a = (15.75 \pm 5.3) - (0.67 \pm 0.1) \log T_a + (0.77 \pm 0.1) \log L_{peak}, \quad (5)$$

where $C_o = (15.75 \pm 5.3)$, $\cos(\phi) \tan(\theta) = (0.67 \pm 0.1)$ and $\sin(\phi) \tan(\theta) = -0.77 \pm 0.1$. All the fits presented in the paper are performed using the D’Agostini method (D’Agostini 2005).

We have quoted the 1σ uncertainties on the coefficients. The intrinsic scatter for the above sample is $\sigma_{int} = 0.27 \pm 0.04$. When we compare it to the $(L_a - T_a)$ correlation for the gold sample, σ_{int} is reduced by 36%. The adjusted R_{adj}^2 for the gold sample is 0.80. R_{adj} gives a modified version of the coefficient of determination, R^2 , adjusting for the number of parameters in the model. $R^2 = 0.81$, the Pearson correlation coefficient is $r = 0.90$ with a probability of the same sample occurring by chance $P = 4.41 \times 10^{-15}$. The normalization of the plane, $C(\sigma_{int}, \phi, \theta)$, is given by:

$$C = 18.30 - 59.90\theta^2 - 0.29\sigma_{int} + 0.27\sigma_{int}^2 - 4.11\phi - 0.06\sigma_{int}\phi + 14.97\phi^2 + \theta(92.07 - 0.09\sigma_{int} + 84.85\phi). \quad (6)$$

For the 122 GRB sample, results are:

$$\log L_a = (15.69 \pm 3.8) + (0.67 \pm 0.07) \log L_{peak} - (0.80 \pm 0.07) \log T_a, \quad (7)$$

with $\sigma_{int} = 0.44 \pm 0.03$. Thus, the reduction in σ_{int} from the 3D correlation for the sample of 122 GRBs to the 3D correlation for the gold sample is again 36%. The R_{adj}^2 for this

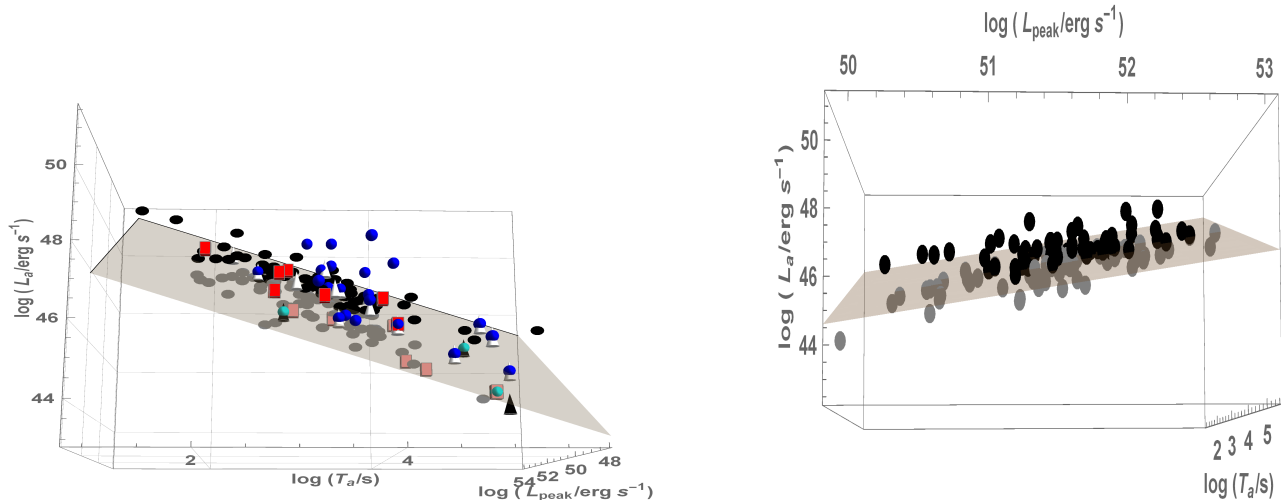


Fig. 2.— The left panel shows the distribution of 176 GRBs in the (L_a, T_a, L_{peak}) space, with the fitted fundamental plane including GRB-SNe (white cones), X-ray flashes (blue spheres), short GRBs with extended emission (red cuboid) and long standard GRBs (black circles). The right panel shows a much tighter plane which results by including only the 122 long GRB sample. The gray and black circles are GRBs which lie below and above the plane respectively.

distribution is 0.56, $R^2 = 0.57$, $r = 0.93$ with $P \leq 2.2 \times 10^{-16}$. Finally, the σ_{int} scatter of the 3D correlation for the gold sample is 54% smaller than the one in the 2D correlation for the 122 GRB sample.

The fundamental plane can be visualized edge on in an infinite number of projections, according to how the projection angle is rotated. However, it is useful to choose a projection where the fundamental plane is seen edge on and one of the axes contains only one of the three relevant parameters. One such option is given in the right panel of figure (3), which shows the fundamental plane for the gold sample. By comparing it with figure (2), and noting the change in scales, it is obvious that the intrinsic scatter has been substantially reduced.

To analyze the distributions of GRBs about the plane, we compute the geometric distance, $\Delta = \sqrt{\Delta_{L_a}^2 + \Delta_{T_a}^2 + \Delta_{L_{peak}}^2}$, where Δ_{L_a} , Δ_{T_a} and $\Delta_{L_{peak}}$ are the distances from the plane of the L_a, T_a and L_{peak} values of each GRB respectively (note that we use dimensionless units for the variables considered). In figure (4) we present a histogram showing the distribution of distances to the fundamental plane for the 122 GRB sample and the gold sample. We note that the gold sample is less scattered about the plane than the 122 GRB sample. The above result is not due to the reduced sample size, as checked by 10^4 Monte

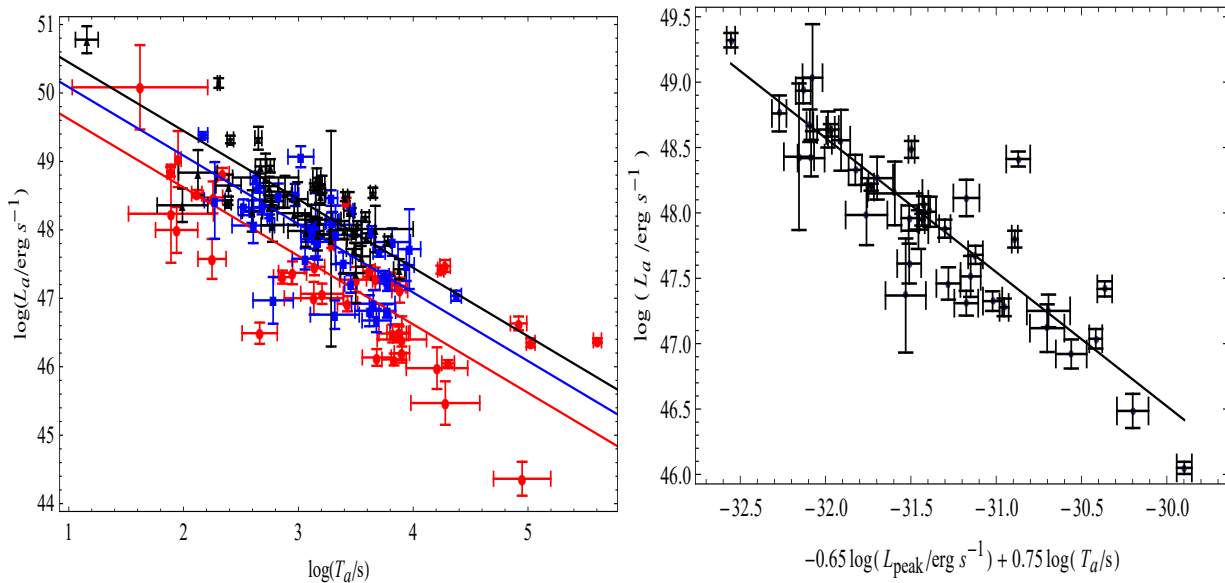


Fig. 3.— Left panel: the (L_a, T_a) plane with error bars, binned into 3 equally populated L_{peak} ranges; $49.9 \leq \log L_{peak} \leq 51.4$ (red circles), $51.4 \leq \log L_{peak} \leq 51.8$ (blue squares) and $51.8 \leq \log L_{peak} \leq 53.0$ (black triangles). The right panel shows the edge-on projection along the intrinsic plane for the three parameter correlation (L_a, T_a, L_{peak}) for the gold sample.

Carlo simulations using bootstrapping of 40 GRBs from the total sample. The probability of obtaining such a random sample having an intrinsic scatter $\sigma_{int} \leq 0.27$ is of 0.3%.

4. Discussion and comparison with other extended $L_a - T_a$ correlations

To derive some insights into the physical nature of the link between prompt and afterglow parameters evident in the fundamental plane obtained, we explore the relation between a proxy of the plateau energy, $L_a T_a$ and L_{peak} . In figure (5) we show the gold sample data points in a $(L_a T_a, L_{peak})$ plane. The $L_a T_a$ show a proportionality to the values of L_{peak} , $(L_a T_a) \propto L_{peak}^{0.59}$, with a Pearson correlation coefficient, $r = 0.60$ and $P = 1.9 \times 10^{-13}$ for the gold sample, while $r = 0.70$ and $P = 4.2 \times 10^{-7}$ for the 122 GRBs. This result demonstrates that the prompt kinetic power is strongly correlated with the plateau energy, for the well-defined plateau exhibiting GRBs. The best fit slope with $\sigma_{int} = 0.29$ is:

$$\log(L_a T_a) = 20.63 + 0.59 \log(L_{peak}) \quad (8)$$

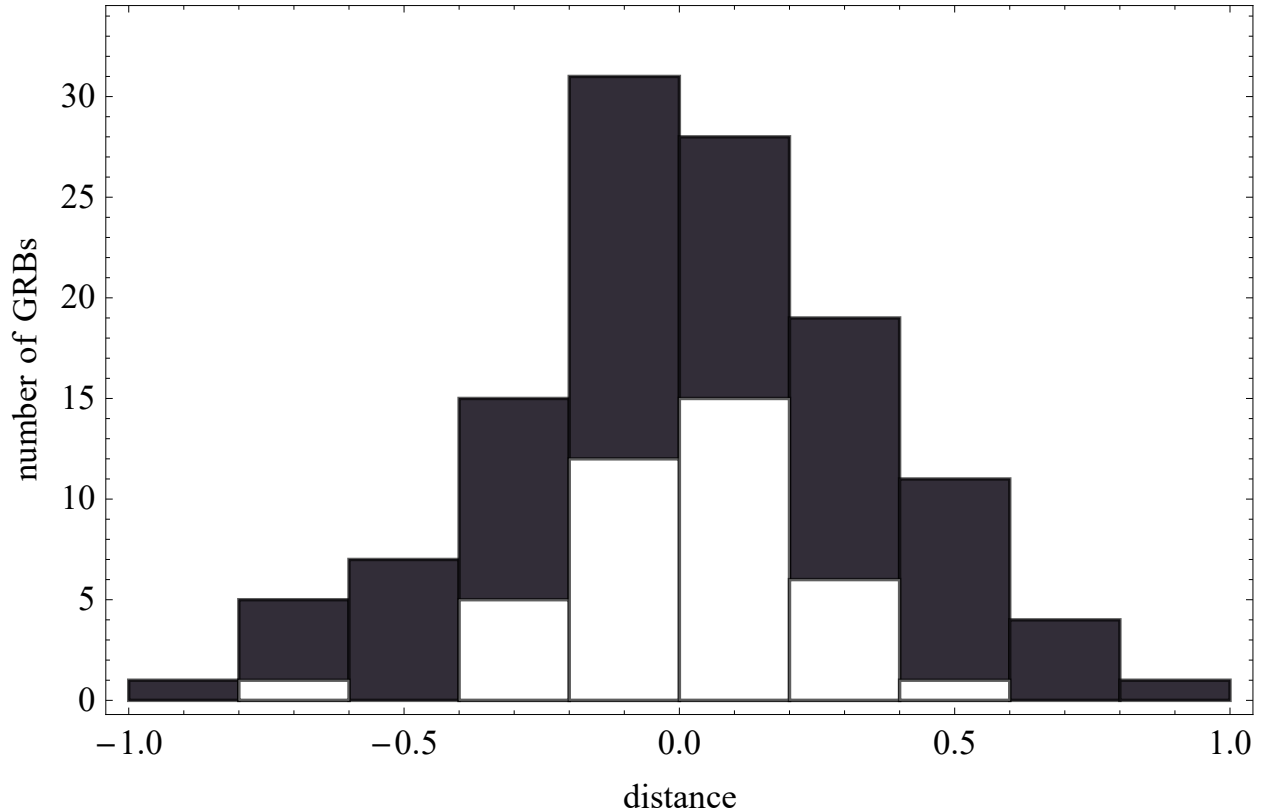


Fig. 4.— Histogram with GRB distances, Δ , to the best fit plane with different shading for gold (white) and non-gold (black) GRBs. The histogram for the 122 long GRBs includes both gold and non-gold members.

We note that this correlation is different from the one presented in Bernardini et al. (2012), where the correlation between the plateau energy and two additional parameters, E_{peak} and E_{iso} is explored yielding $\sigma_{int} = (0.31 \pm 0.03)$. We also note that another fundamental plane ($L_{peak} - E_{iso} - E_{peak}$) has been previously defined, but only amongst prompt emission parameters (Tsutsui et al. 2009). We now compare the $L_a - T_a - L_{peak}$ correlation with other three parameter correlations in the literature, which are extensions of the $L_a - T_a$ correlation. Xu & Huang (2011) showed that adding to the $L_a - T_a$ correlation a third parameter, $E_{iso}(erg)$, the isotropic energy in the prompt emission, results in a significantly tighter ($L_a - T_a - E_{iso}$) correlation with $\sigma_{int} = 0.43$, as compared to the ($L_a - T_a$) one which yields $\sigma_{int} = 0.85$, for their particular chosen sample. When we compare our results to the three parameter correlation found by Xu & Huang (2011) in the (L_a, T_a, E_{iso}) plane, we note that the σ_{int} of our (L_a, T_a, L_{peak}) plane is smaller by 37%. Thus, we can conclude that the 3-parameter correlation introduced here is an improvement on the $L_a - T_a$ correlation as well as on the (L_a, T_a, E_{iso}) correlation.

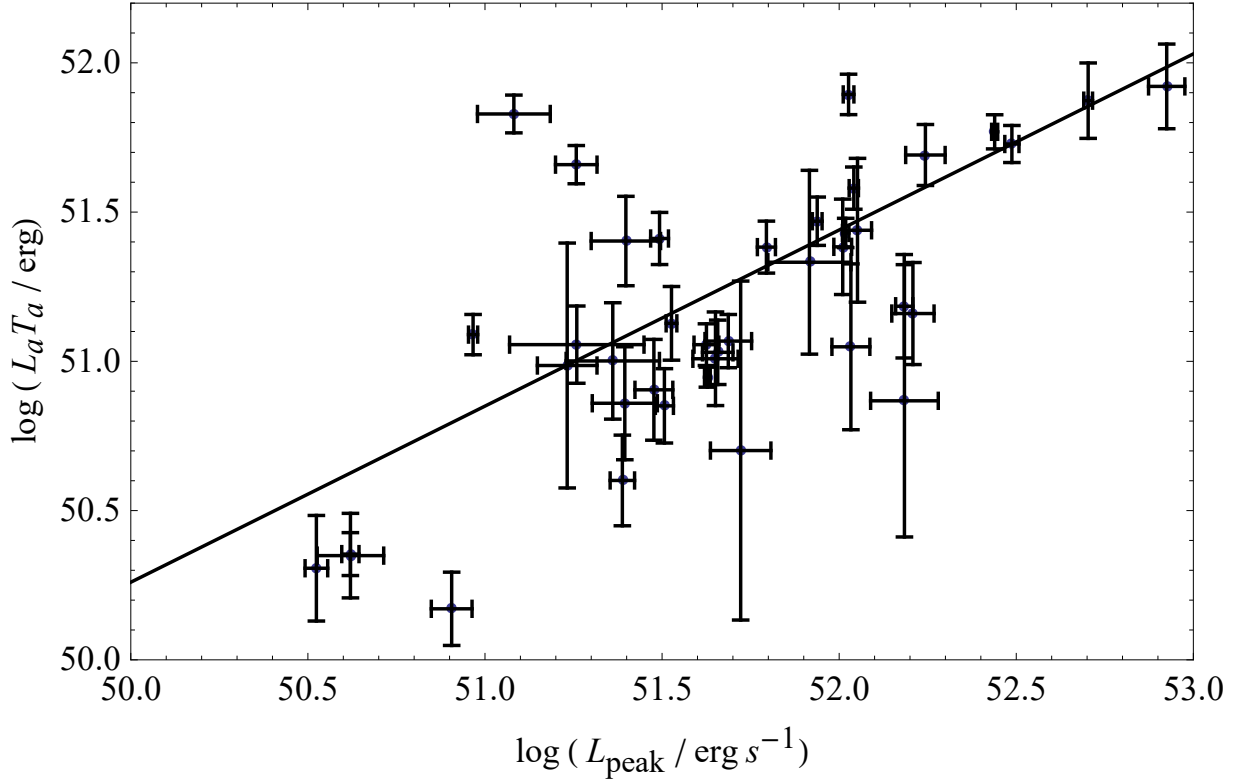


Fig. 5.— $(L_a T_a, L_{peak})$ distribution for the 40 GRBs in the gold GRB sample.

In fact, in Dainotti et al. (2011b) some of us showed that $L_a - L_{iso}$, taking $L_{iso} = E_{iso}/T_{90}$ or $L_{iso} = E_{iso}/T_{45}$, correlates better than $L_a - E_{iso}$ ³. Actually, Dainotti et al. (2015b) demonstrated that the $L_{peak} - L_a$ correlation has a higher correlation coefficient than the $L_{iso} - L_a$ one, showing that L_{peak} is more tightly related to L_a than to any other prompt L_{iso} . The above strongly suggests including L_{peak} and not E_{iso} as a third parameter in the search for a three parameter correlation. Indeed, Dainotti et al. (2015b) have demonstrated through the Efron and Petrosian (1992) method, that the $L_a - L_{peak}$ correlation is intrinsic and not due to any selection bias. Thus, from the intrinsic nature of the $L_{peak} - L_a$ and the $L_a - T_a$ correlations, it follows that the (L_a, T_a, L_{peak}) correlation is also intrinsic.

In addition, we compare our results to an extension of the $L_a - T_a$ correlation (T_a, L_a, E_{peak}) presented in Izzo et al. (2015) where a dispersion of $\sigma_{int} = 0.34$ appears. This scatter is

³where T_{90} and T_{45} are the time intervals over which between 5% and 95% and between 5% and 45% respectively of the total prompt energy is emitted

larger than the $\sigma_{int} = 0.27$ we obtain for the (L_a, T_a, L_{peak}) plane by 21%, thus showing again that L_{peak} is a more suitable variable than E_{peak} . In addition, E_{peak} can introduce biases due to threshold limits both at low and high energies, as discussed in Llyod & Petrosian (1999).

To conclude, through considering a well-defined sub sample of *Swift* GRBs with known redshifts we isolate single class objects. For a well-defined set of 40 such GRBs we obtain a three parameter correlation which is significantly tighter (54%) than what is obtained for the total sample of 122 GRBs with the Dainotti et al. (2016) 2D parameter correlation. The correlation given by $\log L_a = 15.75 + 0.67 \log L_{peak} - 0.78 \log T_a$ can be a useful tool to reduce the uncertainties in inferred cosmological parameters in the high redshift range accessible only to GRBs and can further constrain GRB physical models.

5. Acknowledgments

This work made use of data supplied by the UK Swift Science Data Centre at the University of Leicester. M.G.D acknowledges the Marie Curie Program, because the research leading to these results has received funding from the European Union Seventh Framework Program (FP7-2007/2013) under grant agreement N 626267. M. O. acknowledges the Polish National Science Centre through the grant DEC-2012/04/A/ST9/00083. X. H. acknowledges UNAM-DGAPA IN100814 and CONACyT.

REFERENCES

- Amati, L. et al. A&A, 2009 508, 173.
- Avni, Y. 1976, ApJ, 210, 642
- Bernardini, M.G. et al. 2012, A&A, 539, 3.
- Bernardini, M.G. et al. 2013, ApJ, 775, 67.
- Cardone, V.F. et al. 2009, MNRAS, 400, 775.
- Cardone, V.F., et al. 2010, MNRAS, 408, 1181.
- Cabrera, J. I., et al. 2007, MNRAS, 382, 342.
- Cannizzo, J. K. & Gehrels, N., 2009, ApJ, 700, 1047.
- Cannizzo, J. K., et al. 2011, ApJ, 734, 35.

- Collazzi, A. C., & Schaefer, B. E. 2008 *ApJ*, 688, 456.
- Cucchiara, N. et al. 2011, *ApJ*, 736, 7.
- D' Agostini, G. 2005, arXiv : physics/0511182
- Dall'Osso, S. et al. 2011, *A&A*, 526A, 121D
- Dainotti, M. G. et al. 2008, *MNRAS* 391L, 79.
- Dainotti, M.G. et al. 2010, *ApJL*, 722, L215.
- Dainotti, M. G. et al. 2011a, *ApJ*, 730, 135.
- Dainotti, M.G. et al. 2011b, *MNRAS*, 418, 2202.
- Dainotti, M.G., et al. 2013, *ApJ*, 774, 157.
- Dainotti, M.G., et al. 2013b, *MNRAS*, 436, 82.
- Dainotti, M.G., et al. 2015a, *ApJ*, 800, 31.
- Dainotti, M.G., et al. 2015b, *MNRAS*, 451, 4.
- Evans, P. et al. *MNRAS*, 2009, 397, 1177.
- Efron, B. & Petrosian, V., 1992, *ApJ*, 399, 345.
- Gerhels, N. et al. 2004, *ApJ*, 611, 1005.
- Ghirlanda, G., et al. 2004, *ApJ*, 616, 331.
- Ghisellini, G., et al. 2008, *A&A*, 496, 3, 2009.
- Kouveliotou, C., et al. 1993, *ApJ*, 413, L101.
- Izzo, et al. 2015, *A&A*, 582A, 115.
- Lloyd, N., & Petrosian, V. *ApJ*, 1999, 511, 550.
- Yonetoku, D. et al. 2004, *ApJ*, 609, 935.
- Norris, J.P & Bonnell, J.T. 2006, *ApJ*, 643, 266.
- O' Brien, P.T., Willingale, R., Osborne, J. et al. 2006, *ApJ*, 647, 1213.
- O' Brien, P.T. & Rowlinson, A., 2012, *IAUS*, 279, 297O.

- Rowlinson, A. et al., 2013, MNRAS, 430, 1061.
- Rowlinson, A. et al. 2014, MNRAS, 443, 1779.
- Oates, S. et al. 2012, MNRAS, 426L,86.
- Petrosian, V. & Lloyd, N. 1998, AAS, 193, 8702.
- Petrosian, V. et al. 1999 ASPC, 190, 235.
- Postnikov, S., et al., 2014, ApJ, 783,126.
- Qi, S., Lu, T., & Wang, F.-Y., 2009, MNRAS, 398, L78
- Nanda, R . et al. 2015, ApJ 813, 92.
- Sakamoto, T. et al. 2011, ApJS, 195, 2.
- Schaefer, B. 2007, ApJ, 660, 16.
- Xiao, L. & Schaefer, B.E. 2009, ApJ, 707, 387.
- Tsutsui, R., et al. 2009, JCAP, 08, 015.
- Yamazaki, R. 2009, ApJ, 690, L118.
- M. Xu & Y. F. Huang, A&A 2012, 538, 134.
- Willingale, R. W. et al., ApJ, 2007, 662, 1093.
- Willingale, R. et al. 2010, MNRAS, 403, 1296.
- Zhang, B & Mészáros, P. 2001, ApJ, 552L, 35.